

Room-Temperature Ammonia Formation from Dinitrogen on a Reduced Mesoporous Titanium Oxide Surface with Metallic Properties

Melissa Vettrano, Michel Trudeau,[†] Andy Y. H. Lo, Robert W. Schurko, and David Antonelli*

Contribution from the Department of Chemistry and Biochemistry, The University of Windsor, 401 Sunset Avenue, Windsor, Ontario, Canada N9B-3P4, and Emerging Technologies, Hydro-Québec Research Institute, 1800 Boul. Lionel-Boulet, Varennes, Québec, Canada J3X 1S1

Received February 28, 2002

Abstract: Mesoporous titanium oxide was treated with bis(toluene) titanium under nitrogen at room temperature in toluene, leading to a new blue black material possessing conductivity values of up to $10^{-2} \Omega^{-1} \text{cm}^{-1}$. XRD and nitrogen adsorption showed that the mesostructure was fully retained. Elemental analysis indicated that the material absorbed Ti from the organometallic, without any incorporation of the toluene ligand. There was also an increase of nitrogen from below the detection limit to 1.16%. XPS studies showed that the Ti framework was reduced by the organometallic and that the material had reduced nitride on the surface. There was also an emission at the Fermi level, suggesting metallic behavior. This was confirmed by variable-temperature conductivity studies, which showed a gradual decrease of resistivity with temperature. SQUID magnetometer studies revealed spin glass behavior with a degree of temperature independent paramagnetism, consistent with metallic properties. Solid-state ^{15}N NMR studies on materials synthesized in the presence of labeled dinitrogen showed that the source of the nitride was the reaction atmosphere. IR and ^{15}N NMR demonstrated that this nitrogen species was surface ammonia, suggesting that the initially formed nitride species had reacted with moisture imbedded in the walls of the mesostructure. The direct conversion of dinitrogen to ammonia is a very rare process and this work represents the first example of this process mediated by a molecular sieve.

Introduction

The synthesis of porous materials with tailored properties is one of the most active areas of materials science.^{1–6} In 1992 researchers at Mobil reported the synthesis of the silica MCM-41, the first example of a material with regular pore channels in the 20–100 Å range.⁷ These materials were synthesized by a liquid crystal templating mechanism,^{8–10} and this technique was quickly extended to the fabrication of stable mesoporous transition metal oxides,¹¹ predicted to have advantages over the

analogous silicas in areas such as catalysis, where variable oxidation states are necessary for high activities. In 1999 we demonstrated that mesoporous Nb, Ti, and Ta oxides can act as electron acceptors¹² with a wide variety of electron-transfer reagents to leave materials with nonstoichiometric molecular wires or magnetic phases in the pores.^{13–15} More recently we showed that bis(toluene) niobium deposits a thin layer of low-valent niobium oxide over the surface of mesoporous niobium oxide, providing the first example of a porous oxide with metallic properties. The high reactivity of this new material was demonstrated by a room-temperature dinitrogen cleavage reaction in which surface nitride is formed.¹⁶ This is an extremely

* Corresponding author. E-mail: danton@uwindsor.ca.

[†] Hydro-Québec Research Institute.

- (1) Davis, M. E. *Nature* **1993**, *364*, 391.
- (2) Antonietti, M.; Berton, B.; Goeltner, C.; Hentze, H. *Adv. Mater.* **1998**, *10*, 154.
- (3) Zhao, D.; Feng, J.; Huo, Q.; Melosh, N.; Frederickson, G. H.; Chmelka, B. F.; Stucky, G. D. *Science* **1998**, *279*, 548.
- (4) Holland, B. T.; Blanford, C. F.; Stein, A. *Science* **1998**, *281*, 538.
- (5) Wijnhoven, J. E. G. J.; Vos, W. L. *Science* **1998**, *281*, 802.
- (6) Imhof, A.; Pine, D. J. *Nature* **1997**, *389*, 948.
- (7) (a) Kresge, C. T.; Leonowicz, M. E.; Roth, W. J.; Vartuli, J. C.; Beck, J. S. *Nature* **1992**, *359*, 710. (b) Beck, J. S.; Vartuli, J. C.; Roth, W. J.; Leonowicz, M. E.; Kresge, C. T.; Schmitt, K. D.; Chu, C. T.-W.; Olson, D. H.; Shepard, E. W.; McCullen, S. B.; Higgins, J. B.; Schlenker, J. L. *J. Am. Chem. Soc.* **1992**, *114*, 10834.
- (8) (a) Huo, Q.; Margolese, D. I.; Ciesla, U.; Demuth, D. G.; Feng, P.; Gier, T. E.; Sieger, P.; Firouzi, A.; Chmelka, B. F.; Schuth, F.; Stucky, G. D. *Chem. Mater.* **1994**, *6*, 1176. (b) Firouzi, A.; Kumar, D.; Bull, L. M.; Besier, T.; Sieger, P.; Huo, Q.; Walker, S. A.; Zasadzinski, J. A.; Glinka, C.; Nicol, J.; Margolese, D.; Stucky, G. D.; Chmelka, B. F. *Science* **1995**, *267*, 1138.
- (9) Chen, C.-Y.; Burkette, S. L.; Li, H.-X.; Davis, M. E. *Micropor. Mater.* **1993**, *2*, 27.
- (10) Tanev, P. T.; Chibwe, M.; Pinnavaia, T. J. *Nature* **1994**, *368*, 321.
- (11) Antonelli, D. M.; Ying, J. Y. *Curr. Opin. Colloid Interface Sci.* **1996**, *1*, 523. (b) Antonelli, D. M.; Ying, J. Y. *Angew. Chem., Int. Ed. Engl.* **1995**, *34*, 2014. (c) Antonelli, D. M.; Ying, J. Y. *Angew. Chem., Int. Ed. Engl.* **1996**, *35*, 426. (d) Antonelli, D. M.; Nakahira, A.; Ying, J. Y. *Inorg. Chem.* **1996**, *35*, 3126. (e) Antonelli, D. M.; Ying, J. Y. *Chem. Mater.* **1996**, *8*, 874.
- (12) Vettrano, M.; Trudeau, M.; Antonelli, D. M. *Adv. Mater.* **2000**, *12*, 337. (b) Vettrano, M.; Trudeau, M.; Antonelli, D. M. *Inorg. Chem.* **2001**, *40*, 2088.
- (13) Ye, B.; Trudeau, M.; Antonelli, D. M. *Adv. Mater.* **2001**, *13*, 29. (b) Ye, B.; Trudeau, M.; Antonelli, D. M. *Adv. Mater.* **2001**, *13*, 561.
- (14) Murray, S.; Trudeau, M.; Antonelli, D. M. *Adv. Mater.* **2000**, *12*, 339.
- (15) He, X., and Antonelli, D. M. *Angew. Chem., Int. Ed.* **2002**, *41*, 215–229. (b) He, X.; Trudeau, M.; Antonelli, D. M. *Adv. Mater.* **2000**, *12*, 1036. (c) He, X.; Trudeau, M.; Antonelli, D. M. *Chem. Mater.* **2001**, *13*, 4808. (d) He, X.; Trudeau, M.; Antonelli, D. M. *Inorg. Chem.* **2001**, *40*, 2730.
- (16) Vettrano, M.; He, X.; Trudeau, M.; Antonelli, D. M. *Adv. Funct. Mater.* **2002**, *12*, 174.

rare process^{17–23} and may represent the first step in the development of a new class of catalysts for room-temperature nitrogen reduction or incorporation reactions. In this report we show that mesoporous titanium oxide reacts with bis(toluene) titanium in a nitrogen atmosphere to give surface ammonia, most likely via an initial reductive cleavage by the reduced titania mesostructure, followed by hydrolysis of the nitride by water embedded below the inner surface of the mesostructure. This is the first example of conversion of dinitrogen to ammonia mediated by a molecular sieve. While many electropositive metals react with dinitrogen to form an inert nitride coat, the ease of protonation of the surface nitride in this system suggests that it may be ideal for the development of nitrogen reduction catalysts that may offer superior properties to those already in use.²⁴

Experimental Section

Materials. All chemicals, unless otherwise stated, were obtained from Aldrich. Silver paste was obtained from Alfa-Aesar. The solvent was removed in vacuo and replaced with dry, degassed THF. Samples of mesoporous titanium oxide (Ti-TMS1) were obtained from Alfa-Aesar and used without further purification. Mesoporous titanium oxide samples were dried at 150 °C overnight under vacuum and then treated with trimethylsilyl chloride in diethyl ether at room temperature for 4 h. Bis(toluene) titanium was prepared by metal vapor synthesis with the assistance of Professor F. G. N. Cloke at the University of Sussex.²⁵ Labeled ¹⁵N₂ was obtained from Cambridge Isotopes and used without further purification.

Methods. Nitrogen adsorption and desorption data were collected on a Micromeritics ASAP 2010. X-ray powder diffraction (XRD) patterns (Cu K α) were recorded in a sealed glass capillary on a Siemens D-500 θ - 2θ diffractometer. All X-ray photoelectron spectroscopy (XPS) data were obtained with a Physical Electronics PHI-5500 spectrometer using charge neutralization. All emissions were referenced to the carbon C-(C,H) peak at 284.8 eV. The room-temperature conductivity measurements were recorded on a Jandel four-point universal probe head combined with a Jandel resistivity unit. The equation used for calculating the resistivity was $\rho = 2\pi(S)V/I$, where ρ = resistivity, $\pi/\log n^2$ = sheet resistivity, V = volts, I = current, t = thickness of the pellet, and S = the spacing of the probes (0.1 cm). Variable-temperature resistivity measurements were done by pressing pellets of the material and affixing four copper wires with conducting silver paste, followed by coating the ensemble with epoxy resin. The powder electron paramagnetic resonance (EPR) samples were prepared under vacuum and the data collected on a Bruker X-band ESP 300E EPR spectrometer. Variable-temperature conductivity and magnetic measurements were conducted on a Quantum Design SQUID magnetometer MPMS system with a 5 T magnet. All elemental analysis data (conducted under an inert atmosphere) were obtained from Galbraith Laboratories, Knoxville, TN. Solid-state ¹⁵N MAS and CPMAS NMR experiments were conducted at $\nu_0 = 40.5$ MHz (9.4 T) on a Varian Infinity Plus wide-bore NMR spectrometer at room temperature. All of the samples were powdered and packed into 4 mm o.d. zirconium oxide rotors, with a specially constructed airtight Teflon cap used for air-sensitive materials. The spinning frequencies of both MAS and CPMAS experiments were

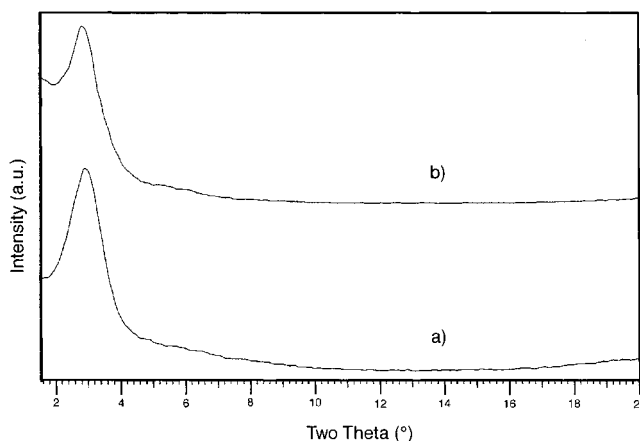


Figure 1. XRD patterns of (a) mesoporous titanium oxide with a 24 Å pore size and (b) sample from part a after treatment with excess bis(toluene) titanium in toluene under dinitrogen.

5 kHz and a high-power broadband ¹H decoupling field of 62.5 kHz was applied. All ¹⁵N NMR spectra were referenced with respect to liquid NH₃ (20 °C), δ iso = 0.0 ppm, by setting the isotropic ammonium ¹⁵N NMR peak of crystalline ¹⁵NH₄¹⁵NO₃ to 23.8 ppm.²⁶ For the CP experiments, the optimized contact times ranged from 3 to 9 ms. The 90° pulses used in the ¹⁵N experiments ranged from 3.4 to 4.4 μ s, with an applied rf field of $\nu_1 = 55$ –74 kHz. ¹⁵N CPMAS NMR spectra were acquired with ca. 200–2000 scans, and MAS NMR experiments with 200–1000 scans.

Synthesis. Excess bis(toluene) titanium, as calculated on the basis of metal percent derived from the elemental analysis data, was added to a suspension of mesoporous titanium oxide in dry toluene under nitrogen. The mesoporous solid immediately went from a light faun color to a deep blue-black. After 1 day of additional stirring to ensure complete absorption of the organometallic, the reduced material was collected by suction filtration under nitrogen and washed several times with toluene. The resulting blue black material was dried in vacuo at 10⁻³ Torr on a Schlenk line until all condensable volatiles had been removed. Samples of mesoporous titanium oxide treated with ammonia or ammonium for use as spectroscopic references were prepared by vapor diffusion or solution impregnation in methanol/water.

Results and Discussion

A sample of trimethylsilylated mesoporous titanium oxide, possessing a BET (Brunauer, Emmett, Teller) surface area of 785 m² g⁻¹, an HK pore size of 24 Å, and an X-ray powder diffraction (XRD) pattern displaying one peak centered at $d = 32$ Å, was treated with excess bis(toluene) titanium in toluene over 24 h until absorption was judged complete. The new blue-black material was collected by suction filtration, washed with excess toluene, and dried in vacuo. Generally about 1.3 weight equivalents of the organometallic were absorbed per weight equivalent of the mesoporous oxide. The XRD pattern of this air-sensitive solid displayed a broad peak centered at $d = 32$ Å (Figure 1) while the BET surface area dropped to 507 m² g⁻¹ and the HK (Horvath–Kawazoe) pore size decreased to 19 Å (Figure 2). The elemental analysis of this new material gave 51.13% Ti, 2.56% C, 1.07% H, 0.62% Si, and 1.16% N as compared to 38.11% Ti, 3.12% C, 1.36% H, 0.94% Si, and <0.01% N in the starting material. From these data a molecular formula of Ti_{1.0}O_{2.5}C_{0.2}H_{1.0}N_{0.08}Si_{0.02} can be calculated. The

(17) Laplaza, C. E.; Cummins, C. C. *Science* **1995**, *268*, 861.

(18) Niewa, R.; Jacobs, H. *Chem. Rev.* **1996**, *96*, 2053.

(19) Niewa, R.; DiSalvo, F. J. *Chem. Mater.* **1998**, *10*, 2733.

(20) Leigh, G. L. *Acc. Chem. Res.* **1992**, *25*, 177.

(21) Manriquez, J. M.; Bercaw, J. E. *J. Am. Chem. Soc.* **1974**, *96*, 6229.

(22) Fryzuk, M. D.; Love, J. B.; Rettig, S. J.; Young, V. G. *Science* **1997**, *275*, 1445.

(23) Asahi, R.; Morikawa, T.; Ohwaki, T.; Aoki, K.; Taga, Y. *Science* **2001**, *293*, 269.

(24) Kubota, J.; Aika, K. *J. Phys. Chem.* **1994**, *98*, 11293.

(25) Cloke, F. G. N. *Chem. Soc. Rev.* **1993**, *17*.

(26) Hayashi, S.; Hayamizu, K. *Bull. Chem. Soc. Jpn.* **1991**, *64*, 688. (b) Witanowski, M.; Stefaniak, L.; Webb, G. A. *Annu. Rep. NMR Spectrosc.* **1993**, *25*, 1.

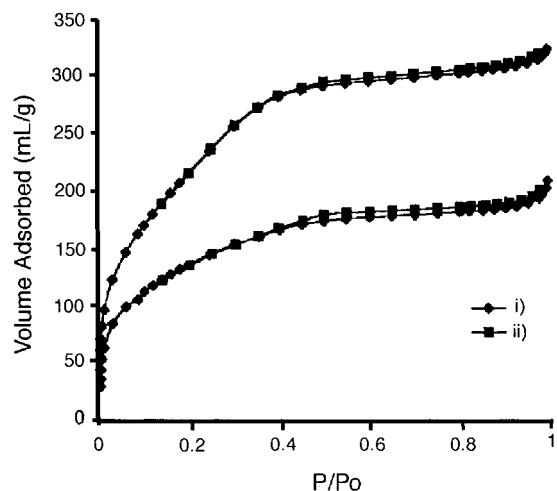


Figure 2. Nitrogen adsorption(i)–desorption(ii) isotherms of samples from Figure 1 (a) (upper curve) and (b) (lower curve).

increase in Ti with a small decrease in the C suggests that the bis(toluene) titanium lost the toluene ligand and acted as a Ti atom donor to the mesostructure, leaving a thin layer of a new Ti species on the surface of the pore channels. The thermal decomposition of bis(toluene) titanium over mesoporous aluminum oxide has been used previously as a method of depositing nanoscale grains of Ti metal in the pores of the alumina;²⁷ however, our approach differs as decomposition is likely induced by oxidation of the organometallic Ti(0) complex by the Ti (IV) mesostructure, since bis(toluene) titanium is thermally stable at room temperature.²⁵ A similar oxidative decomposition was confirmed by XPS in previous studies on the closely analogous reduction of mesoporous niobium oxide by bis(toluene) niobium.¹⁶ The most salient feature of the elemental analysis, however, is the incorporation of 1.16% N in the material, since the only nitrogen source present in the synthesis conditions was N₂, an extremely robust molecule that is notoriously difficult to activate. The IR spectrum shows a broad absorbance centered at 3410 cm⁻¹ that can be assigned to moisture embedded in the walls of the mesostructure, as well as a smaller broad absorbance at 3180 cm⁻¹ suggestive of a hydrogen-bonded N–H species. In a previous report we showed that mesoporous niobium oxide treated with bis(toluene) niobium under argon led to the formation of a thin film of low-valent Nb(II) species on the surface and that treatment of this material with dinitrogen led to formation of surface nitride.¹⁶ ¹⁵N NMR studies confirmed that the source of the nitride was indeed dinitrogen; however the specific nature of this nitride species was not established. The extension of this chemistry to Ti-based systems represents a significant step, since bis(toluene) niobium is extremely difficult to synthesize²⁵ and Ti is a much less expensive metal than Nb. There is also considerable interest in developing nitrogen-doped titania for use as visible-light photocatalysts.²³

To further probe into the nature of the surface species present in this new reduced mesoporous titanium oxide material, X-ray photoelectron spectroscopy studies were conducted. Figure 3a shows the 3p 1/2,3/2 region of the XPS spectrum of a sample of mesoporous titanium oxide treated with bis(toluene) titanium. The 3p 1/2 emission falls at 37.5 eV, as compared to 36.8 eV in the material reduced with 1.0 equiv of Li and 37.9 eV in the

unreduced material. The gradual shift to lower binding energy on reduction of the framework has been commented on before;¹² in this case the emission at 37.5 eV demonstrates reduction of the framework to a level of about Ti 3.6⁺. There is a shoulder at 35.1 eV corresponding to Ti(II), which is likely associated with the reduced phase on the surface. There is no evidence for Ti metal originating from the organometallic. These data are in accord with analogous mesoporous niobium oxide materials reduced with bis(toluene) niobium under nitrogen, which display two clear emissions in the Nb 3/2,5/2 region corresponding to Nb 4.8⁺ and Nb 2⁺. The N 1s region is also similar to that in the Nb material (Figure 3c), exhibiting emissions at 399.8 and 397.3 eV corresponding to two reduced nitride species. There was no discernible evidence for chemisorbed N₂, which comes at 402 eV. Saha reported peaks at 397.1 and 399.2 eV for samples of partially oxygenated TiN,²⁸ while Guimon et al. reported that ammonia absorbed onto the surface of titanium oxide exhibits N 1s emissions at 400.1 and 402.3 eV for Lewis and Brønsted sites, respectively, and 399.1 eV for surface amide.²⁹ From these values and the IR data, the emission at 399.8 eV in our material can be tentatively assigned to surface ammonia, while the emission at 397.3 eV is due to a second nitride species, the identity of which is not clear. Figure 3b shows the region near the Fermi level of the material reduced with bis(toluene) titanium. The large emission from 3 to 8 eV corresponds to the O 2p valence band electrons, while the smaller hump at the Fermi level is indicative of metallic behavior, common in low-valent early transition metal oxides such as VO, TiO, and NbO.³⁰ Electron transport measurements using the four-point method on pressed pellets of this material show surprisingly high conductivity values of 10⁻² Ω⁻¹ cm⁻¹, over 1000 times greater than the Ti-based materials reduced with 1.0 equiv of Li. The plot of conductivity versus temperature is shown in Figure 4 and displays a slight increase by a factor of 2 on decreasing the temperature to liquid helium values. This behavior is typical of a classical metal. The electron paramagnetic resonance (EPR) spectrum of this material displays one broad resonance centered at 2.0 g that can be assigned to free electrons in the inner walls of the reduced Ti 3.6⁺ mesostructure on the basis of previous work on the EPR spectra of reduced mesoporous Ti oxide species.^{12b} There is a second resonance at higher field, much broader and lower in intensity, which can be assigned to the reduced Ti species on the surface of the material.

Figure 5a shows a plot of the zero field cooled (ZFC) and field cooled (FC) molar magnetization versus temperature for the sample in Figure 3 over a temperature range from 4 to 150 K. The transition at around 20 K in the ZFC branch of the plot is a signature of spin glass behavior, also observed in cobaltocene and nickelocene composites of mesoporous niobium oxide.¹⁵ Above 20 K, the magnetization decreases with increasing temperature according to the Curie law and shows a temperature independent term expected on the basis of the high conductivity and the emission at the Fermi level in the XPS spectrum. Figure 5b shows the plot of molar magnetization versus T⁻¹, exhibiting a Y-intercept at 1.32 × 10⁻² emu, corresponding to the temperature independent paramagnetism.

(28) Saha, N. C.; Tompkins, H. G. *J. Appl. Phys.* **1992**, *72*, 3072.

(29) Guimon, C.; Gervasini, A.; Auroux, A. *J. Phys. Chem. B* **2001**, *105*, 10316.

(30) Cox, P. A. *The Electronic Structure and Chemistry of Solids*; Oxford University Press: New York, 1987.

(27) Schneider, J. *J. Adv. Mater.* **2001**, *13*, 529.

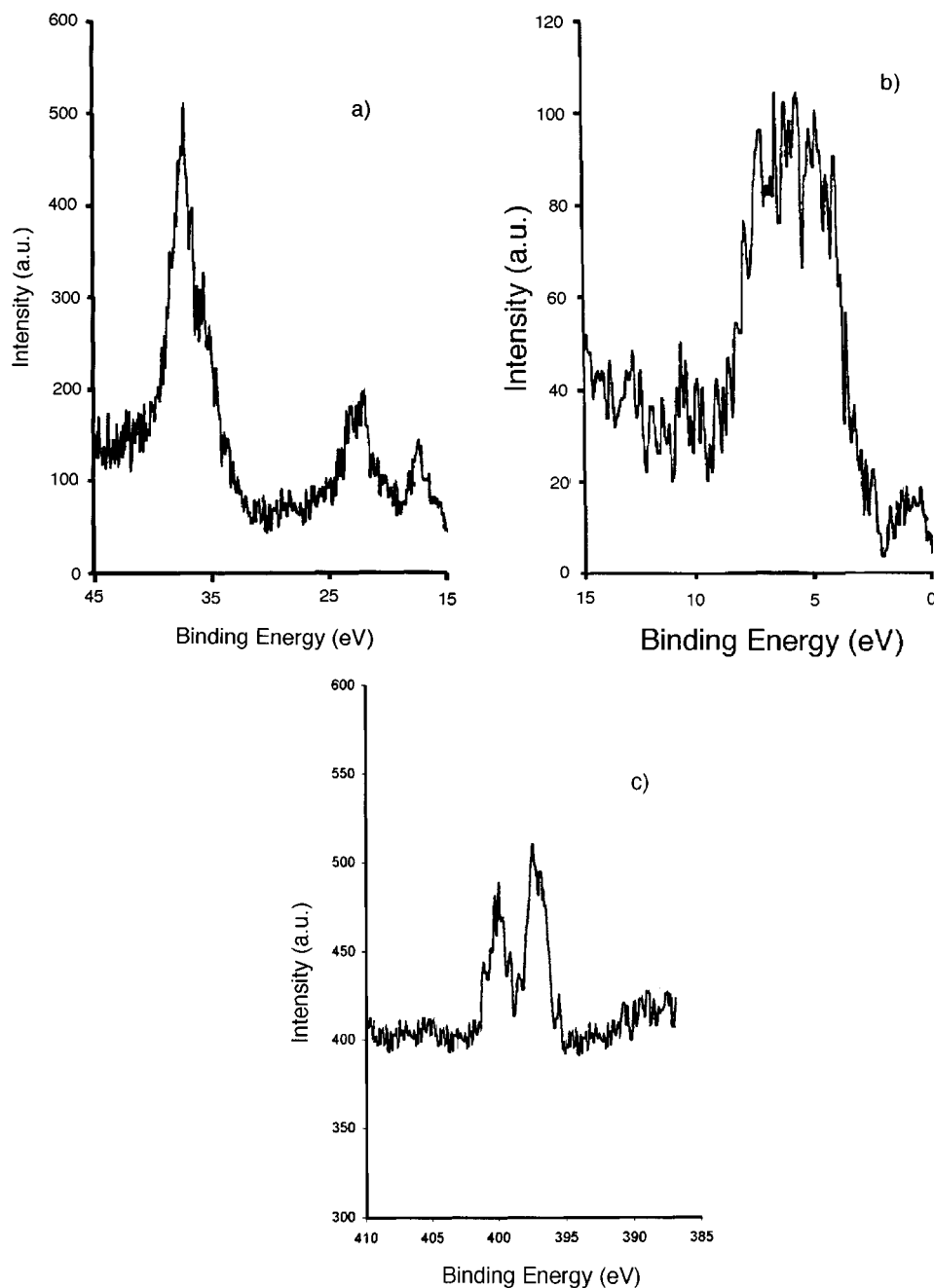


Figure 3. XPS spectrum of mesoporous titanium oxide treated with bis(toluene) titanium under dinitrogen showing (a) the Ti 3p 1/2, 3/2 region, (b) the region near the Fermi level, and (c) N 1s region.

From the temperature dependent branch of these data a μ_{eff} of 2.1 can be calculated, indicative of 1.30 unpaired electrons per stoichiometric unit.³¹ This is in accord with the stoichiometry of the material, which permits a maximum of 1.74 unpaired electrons per Ti center on the basis of the amount of bis(toluene) titanium (d^4) absorbed by the T(IV) (d^0) framework. The difference of 0.44 between these two numbers can be accounted for by the presence of some spin pairing, expected in a composite oxide material showing evidence of both metallic and spin glass behavior.

To confirm that the nitride in the material originated from dinitrogen, the synthesis was carried out on a high vacuum Schlenk line under a ^{15}N atmosphere. After 3 days of stirring to ensure maximum absorption of the nitrogen, the sample was

collected by filtration and dried in vacuo. Figure 6a shows the ^{15}N CPMAS spectrum of this labeled material clearly exhibiting a broad resonance at ca. 26 ppm relative to liquid ammonia, consistent with an aminoid sp^3 hybridized nitrogen.^{11c} The peak positions are similar to those reported previously for mesoporous niobium oxide reduced with bis(toluene) niobium under dinitrogen and differ substantially from those expected for a terminal nitride, which can appear as far downfield as +840 ppm relative to nitromethane (+1220 ppm relative to ammonia).¹⁷ There is no clear resonance for the second nitrogen species observed by XPS, either because it is too broad or because it is coincident with the first nitrogen resonance. The activation of dinitrogen

(31) Chen, C.-W. *Magnetism and Metallurgy of Soft Magnetic Materials*; Dover: New York, 1986.

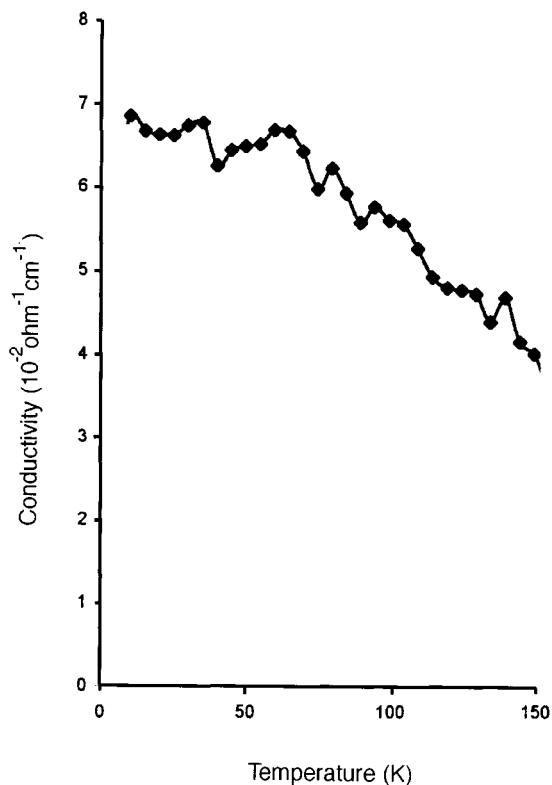


Figure 4. Plot of variable-temperature four-point conductivity measured on epoxy-coated pellets of mesoporous titanium oxide treated with bis-(toluene) titanium.

by a metal oxide is extremely difficult, normally requiring microwave radiation and argon plasmas.^{18,19} We attribute the high reactivity of our material to low-valent, low-coordinate Ti centers on the surface of the material formed by the oxidative decomposition of bis(toluene) titanium on the inner and outer surface of the material. Reductive cleavage of dinitrogen by transition metal complexes is rare; however, the cleavage of dinitrogen by sterically shielded low coordinate d^3 Mo(III) centers proceeds smoothly at room temperature.¹⁷ Since Ti(II) does not have enough electrons to reduce dinitrogen, several adjacent Ti centers must be involved in this process. Many electropositive metals form a thin coating of nitride on the surface upon exposure to air, but these materials are notoriously inert to further reaction of the nitride functionality.

To unequivocally characterize the surface nitrogen species, a combination of $^{15}\text{N}\{^1\text{H}\}$ MAS and CPMAS NMR experiments was conducted. The ^{15}N CPMAS spectrum discussed above is shown in Figure 6a, while the MAS NMR spectra of this material is shown in Figure 6b. In both cases, the NMR powder patterns are very broad (ranging from 500 to 700 Hz at half-height). Spectra acquired under conditions of cross-polarization have higher signal-to-noise ratio than comparable single pulse ^{15}N MAS NMR spectra, by a factor of ca. 1.5–1.7. The isotropic chemical shifts in each spectrum are approximately 25.6(0.8) ppm with respect to liquid ammonia.³² The chemical shift, broad line shape, and high proton CP efficiency suggest that the ^{15}N line shape arises from $^{15}\text{NH}_3$ groups that are anchored to the surface of the mesostructure. The chemical shift is very close

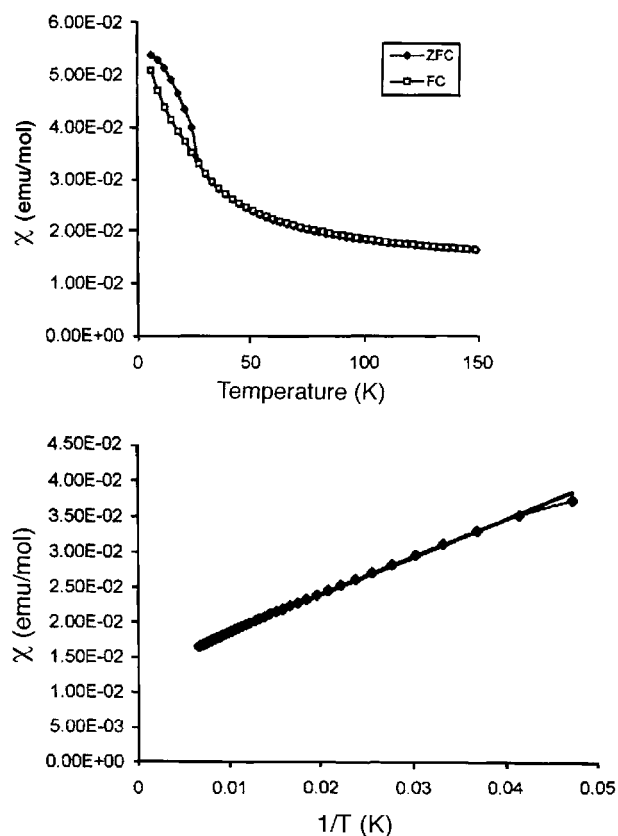


Figure 5. (a) Plot of zero field cooled and field cooled molar magnetic susceptibility versus temperature for a sample of mesoporous titanium oxide treated with bis(toluene) titanium under dinitrogen. (b) Plot of molar magnetic susceptibility versus inverse temperature for the sample from part a.

to the shift of 23.8 ppm for the ammonium ion in NH_4NO_3 , suggesting a tetrahedral nitrogen environment, as opposed to free N_2 ($\delta_{\text{iso}}(^{15}\text{N}) = 310$ ppm),³² TiN ($\delta_{\text{iso}}(^{15}\text{N}) = 400$ ppm),³³ or other oxidized nitrogen species. The broad line shape arises from a distribution of chemical shifts due to the physisorbed NH_3 on the disordered surface of the mesoporous titanium oxide. If the surface-bound ammonia has a strong binding interaction with a paramagnetic niobium atom, it is possible that some of the unpaired electron spin density may be distributed within the molecular orbitals of the ammonia species. The result would be a significant change in ^{15}N chemical shift or broadening (inhomogeneous and/or homogeneous) of the ^{15}N NMR resonances. The observed resonances are not unusually shifted away from the typical range of ^{15}N chemical shifts for ammonia species, nor do they possess large spinning sideband manifolds, indicating a large Knight shift anisotropy; thus, if there is a contribution from unpaired electrons in the lattice to the ^{15}N NMR spectra, it is likely very small and difficult to distinguish from the inhomogeneous line broadening caused by a distribution of chemical shifts in the disordered sample. The fact that the NH_3 is anchored to the surface in this case results in ^{15}N CPMAS NMR spectra that would not be observed if the NH_3 was isotropically tumbling away from the titania surface. Virtually identical NMR spectra have been reported for the absorption of NH_3 on the surface of TiO_2 -supported V_2O_5 catalysts.³⁴

(32) Hayashi, S.; Hayamizu, K. *Bull. Chem. Soc. Jpn.* **1991**, *64*, 688. (b) Witanowski, M.; Stefaniak, L.; Webb, G. A. *Annu. Rep. NMR Spectrosc.* **1993**, *25*, 1.

(33) MacKenzie, K. J. D.; Meinhold, R. H.; McGavin, D. G.; Ripmeester, J. A.; Moudrakovski, I. *Solid State Nucl. Magn. Reson.* **1995**, *4*, 193.

(34) Hu, S.; Apple, T. M. *J. Catal.* **1996**, *158*, 199.

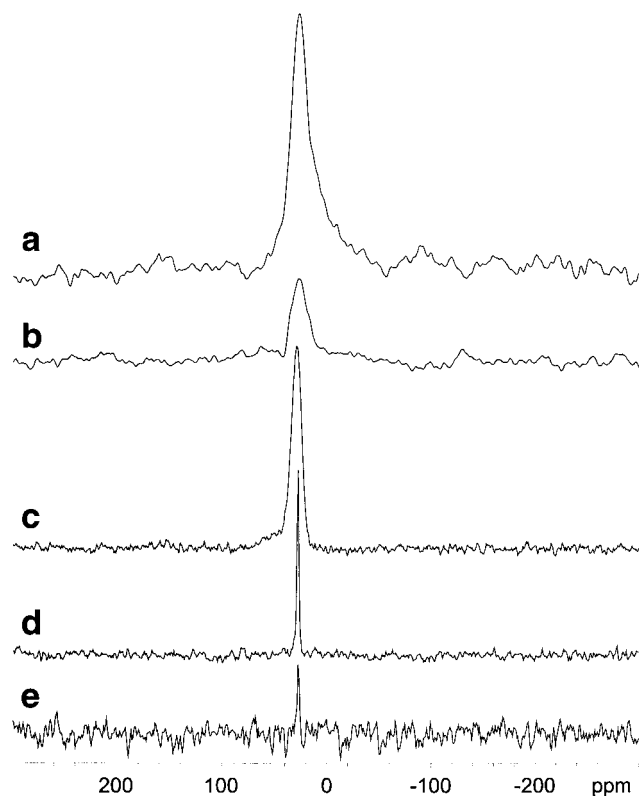


Figure 6. (a) $^{15}\text{N}\{^1\text{H}\}$ CPMAS NMR spectrum of mesoporous titanium oxide treated with bis(toluene)titanium in the presence of $^{15}\text{N}_2$. (b) $^{15}\text{N}\{^1\text{H}\}$ MAS NMR spectrum of the same sample. (c) $^{15}\text{N}\{^1\text{H}\}$ CPMAS NMR spectrum of the above sample exposed to air. (d) $^{15}\text{N}\{^1\text{H}\}$ MAS NMR spectrum of air-exposed sample treated with H_2O . (e) $^{15}\text{N}\{^1\text{H}\}$ CPMAS NMR spectrum of air-exposed sample treated with H_2O .

NMR spectra of a $^{15}\text{N}_2$ -treated sample exposed to varying degrees of air and moisture are compared in parts c–e of Figure 6. In the ^{15}N CPMAS NMR spectrum (Figure 6c) of the sample exposed only to air, a familiar broad peak is centered at 26.5–(1.0) ppm with a slightly reduced line width of 400 Hz compared to the original samples. There is also a broad tail on the peak in the high-frequency direction, suggesting perhaps that a minor reaction has taken place. The XPS of this material shows a slight reduction of the emission at lower binding energy in the N 1s region and an increase of the emission at 399.8 eV. The IR spectrum of this material shows a slight increase in intensity of the absorbance at 3180 cm^{-1} . Again, the high CP efficiency, chemical shift, and the broad line shape imply that the ammonia species remains physisorbed on the titania surface. ^{15}N MAS NMR spectra (Figure 6d) of the sample treated with air and then excess moisture by vapor diffusion over several days reveal a very sharp peak with $\delta_{\text{iso}}(^{15}\text{N}) = 27.1(0.2)$ ppm and a much reduced line width of ca. 80 Hz. The N 1s region of the XPS spectrum shows only the emission at 399.8 eV, while the IR spectrum shows a further increase in the intensity of the absorbance at 3180 cm^{-1} . ^{15}N CPMAS NMR spectra (Figure 6e) acquired with various contact times and pulse delays have very poor signal-to-noise ratio in comparison to corresponding MAS NMR spectra. This is further evidence that $^{15}\text{NH}_3$ has been produced at the titania surface after treatment with $^{15}\text{N}_2$, since surface $^{15}\text{NH}_3$ will react with water to form ammonium ions that are not physisorbed to the surface, and therefore not as amenable to cross polarization as surface-

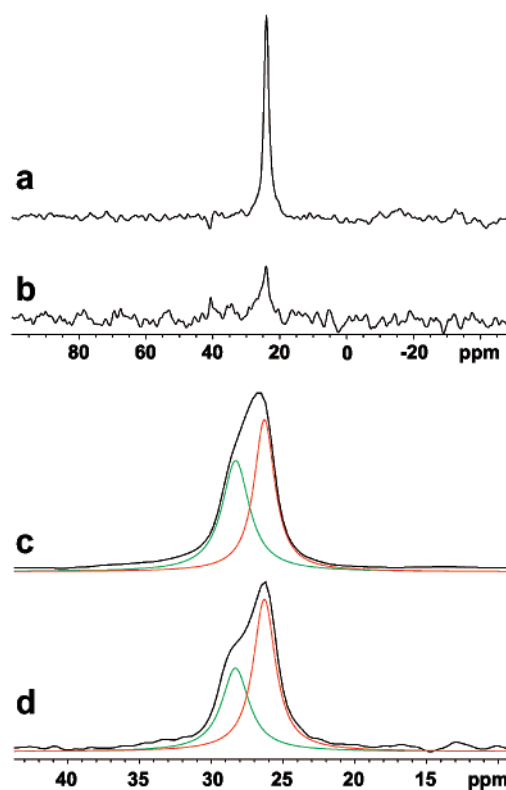


Figure 7. (a) $^{15}\text{N}\{^1\text{H}\}$ MAS and (b) $^{15}\text{N}\{^1\text{H}\}$ CPMAS NMR spectra of mesoporous titanium oxide treated with $^{15}\text{NH}_4\text{NO}_3(\text{aq})$. (c) $^{15}\text{N}\{^1\text{H}\}$ MAS and (d) $^{15}\text{N}\{^1\text{H}\}$ CPMAS NMR spectra of mesoporous titanium oxide treated with NH_3 . Peak deconvolution is shown for parts c and d.

anchored NH_3 . In addition, the loss of the broad line shape indicates that the nitrogen species are undergoing rapid isotropic motion.

To further prove our hypothesis regarding formation of surface NH_3 after treatment with N_2 and reaction with nascent protons, mesoporous titanium oxide materials were treated with isotopically enriched $^{15}\text{NH}_3$ and $^{15}\text{NH}_4\text{NO}_3$. The presence of surface N–H species was confirmed by the presence of a broad IR absorbance centered at 3180 cm^{-1} . The XPS spectrum of these materials was in complete accord to those published previously, displaying emissions in the N 1s region at 402.3 eV for ammonium and 399.9 eV (only in the sample treated with NH_3) for surface ammonia corresponding to values previously quoted for adsorbed ammonia on a titania surface.²⁹ $^{15}\text{N}\{^1\text{H}\}$ MAS and CPMAS NMR spectra are shown in Figure 7. The $^{15}\text{N}\{^1\text{H}\}$ MAS NMR spectrum for titanium oxide treated with $^{15}\text{NH}_4\text{NO}_3$ (Figure 7a) has a single intense narrow peak (fwhh = 50 Hz) with $\delta_{\text{iso}}(^{15}\text{N}) = 22.4(0.2)$ ppm, suggesting the presence of free $^{15}\text{NH}_4^+$ ions. The corresponding $^{15}\text{N}\{^1\text{H}\}$ CPMAS NMR spectrum (Figure 7b) shows very poor cross-polarization efficiency, which is consistent with isotropic tumbling of the $^{15}\text{NH}_4^+$ ions. $^{15}\text{N}\{^1\text{H}\}$ MAS and CPMAS NMR spectra (Figure 7, parts c and d, respectively) of $^{15}\text{NH}_3$ -treated titania both have broad peaks by comparison (ca. 110–130 Hz), with $\delta_{\text{iso}} = 26.3(0.5)$ ppm. Compared to the sample treated with $^{15}\text{NH}_4\text{NO}_3$, the peaks are broadened by an inhomogeneous chemical shift distribution and increased CP efficiency is observed in the ^{15}N CPMAS NMR spectrum. However, the CP efficiency is less than observed for the original $^{15}\text{N}_2$ -treated mesoporous titanium oxide samples (see Figure 6a,b). Decon-

olution of the peaks in Figure 7, parts c and d, gives two peaks at 28.3 and 26.3 ppm in a 1:1 and 3:2 ratio, respectively, for the Lewis and Brønsted adsorption sites discussed above. The slightly different shift for the Brønsted sites with respect to the sample loaded with $^{15}\text{NH}_4\text{NO}_3$ can possibly be accounted for by the different degrees of hydrogen bonding of the ammonia species expected in the two samples.

These NMR studies unequivocally prove that surface ammonia species are present in the materials. The conversion of dinitrogen to ammonia in this system most likely occurs by cleavage of dinitrogen by low valent Ti centers on the surface of the mesostructure followed by reaction with water embedded beneath the surface, which slowly diffuses to the surface of the pore channels. Treatment of this material with excess H_2O leads to disappearance of the XPS N 1s emission at lower binding energy due to the nitride and an increase in the emission due to surface ammonia, effectively completing the hydrolysis of the nitride precursor. Only the materials isolated prior to treatment with moisture display metallic behavior, indicating that much of the surface Ti is still in the reduced form after the initial reaction with dinitrogen. We anticipate that the metallic properties of the surface will facilitate electron transport processes involved in such a process and that the high porosity and ease of desorption of the surface ammonia demonstrated by the NMR studies in this report will be highly advantageous in terms of substrate and product diffusion.

Conclusion

Treatment of mesoporous titanium oxide with bis (toluene) titanium in the presence of ambient nitrogen leads to a low-valent metallic mesostructure with observation of surface ammonia species as confirmed by XPS, IR, and NMR. The formation of ammonia likely proceeds by cleavage of dinitrogen by a low-valent Ti species, followed by reaction with moisture diffusing from beneath the surface of the structure. The high porosity and facile electron transport properties of this material make it an ideal candidate for a catalytic support material for nitrogen reduction and incorporation reactions. Although water is not expected to be a part of a viable catalytic process, the use of hydrogen as a reductant in these reactions is certainly feasible.

Acknowledgment. The Petroleum Research Fund administered by the American Chemical Society and NSERC are acknowledged for funding of this work. The Ontario Premier's Research Excellence Award (PREA) program is also thanked. John Robinson is acknowledged for his help in obtaining XRD data. R. W. Schurko thanks the Canadian Foundation for Innovation, Ontario Innovation Trust, NSERC, and the University of Windsor.

Supporting Information Available: Infrared spectra of all materials discussed and EPR data is also available. This material is available free of charge via the Internet at <http://pubs.acs.org>.

JA020313P